

Effects of ferroelectric-poling-induced strain on the transport and magnetic properties of $\text{La}_{7/8}\text{Ba}_{1/8}\text{MnO}_3$ thin films

R. K. Zheng,^{1,a)} Y. Wang,¹ H. L. W. Chan,¹ C. L. Choy,¹ H.-U. Habermeier,² and H. S. Luo³

¹Department of Applied Physics and Materials Research Center, The Hong Kong Polytechnic University, Hong Kong, China

²Max Planck Institute for Solid State Research, Heisenbergstrasse 1, D-70569 Stuttgart, Germany

³State Key Laboratory of High Performance Ceramics and Superfine Microstructure, Shanghai Institute of Ceramics, Chinese Academy of Sciences, Shanghai 201800, China

(Received 28 May 2010; accepted 12 June 2010; published online 6 August 2010)

We have investigated the effects of the strain induced by ferroelectric poling on the transport and magnetic properties of $\text{La}_{7/8}\text{Ba}_{1/8}\text{MnO}_3$ (LBMO) thin films epitaxially grown on ferroelectric $0.67\text{Pb}(\text{Mg}_{1/3}\text{Nb}_{2/3})\text{O}_3-0.33\text{PbTiO}_3$ (PMN-PT) single-crystal substrates. The ferroelectric poling reduces the in-plane tensile strain of the film, giving rise to a decrease in the resistivity and an increase in the magnetization, Curie temperature, and magnetoresistance of the LBMO film. These strain effects are explained within the framework of coexisting phases whose volume fractions are modified as a result of the reduction in the tetragonal distortion of MnO_6 octahedra induced by ferroelectric poling. An investigation of the effects of polarization reversal on the transport properties of the LBMO film indicates that the ferroelectric-poling-induced strain effects dominate over the ferroelectric field effects in the LBMO/PMN-PT structure. © 2010 American Institute of Physics. [doi:10.1063/1.3464226]

I. INTRODUCTION

The effects of substrate-induced strain on the properties of perovskite manganite thin films are quite complex and still under investigation.¹⁻¹¹ Zhang *et al.*¹ reported that lightly doped $\text{La}_{1-x}\text{Ba}_x\text{MnO}_3$ ($0.05 \leq x \leq 0.2$) thin films show anomalous strain effects, which is different from those previously observed in $\text{La}_{0.9}\text{Sr}_{0.1}\text{MnO}_3$,² $\text{La}_{0.7}\text{Ca}_{0.3}\text{MnO}_3$,³ $\text{Nd}_{0.7}\text{Sr}_{0.3}\text{MnO}_3$,⁴ and $\text{La}_{0.67-x}\text{Pr}_x\text{Ca}_{0.33}\text{MnO}_3$ ($x = 0.13, 0.2, 0.27$) (Ref. 5) thin films. They observed that the substrate-induced in-plane tensile strain dramatically reduces the resistivity and enhances the ferromagnetism and Curie temperature (T_C) of $\text{La}_{1-x}\text{Ba}_x\text{MnO}_3$ ($0.05 \leq x \leq 0.2$) thin films and suggested that the tensile strain-induced stabilization of $d_{x^2-y^2}$ orbital is responsible for the enhanced ferromagnetism and T_C . Using hall measurements, Kanki *et al.*⁶ found that the tensile strain-induced enhancements in ferromagnetism and T_C of $\text{La}_{1-x}\text{Ba}_x\text{MnO}_3$ ($0.05 \leq x \leq 0.2$) thin films are due to enhanced carrier mobility arising from strain-induced modification of Mn-O-Mn network. In contrast, Murugavel *et al.*⁷⁻⁹ reported that, irrespective of whether the substrate-induced strain is compressive or tensile, the oxygen nonstoichiometry, which depends on the oxygen pressure during film deposition and postannealing process, strongly influences the structural, transport, and magnetic properties of the lightly doped $\text{La}_{1-x}\text{Ba}_x\text{MnO}_3$ ($x = 0.08, 0.2$) thin films. Orgiani *et al.*¹⁰ reported similar effects of oxygen nonstoichiometry on the transport properties and T_C of $\text{La}_{0.7}\text{Ba}_{0.3}\text{MnO}_3$ thin films. These results demonstrate

the important role of the oxygen content in determining the structural and physical properties of $\text{La}_{1-x}\text{Ba}_x\text{MnO}_3$ thin films.

In order to obtain further insight into the effects of substrate-induced strain on the transport and magnetic properties of lightly doped $\text{La}_{1-x}\text{Ba}_x\text{MnO}_3$ thin films, we epitaxially grown lightly doped $\text{La}_{7/8}\text{Ba}_{1/8}\text{MnO}_3$ (LBMO) thin films on ferroelectric $0.67\text{Pb}(\text{Mg}_{1/3}\text{Nb}_{2/3})\text{O}_3-0.33\text{PbTiO}_3$ (PMN-PT) single-crystal substrates and *in situ* dynamically reduces the in-plane tensile strain of the LBMO film via ferroelectric poling, such that the effects of extrinsic variables such as oxygen nonstoichiometry are kept constant since we used the same piece of LBMO/PMN-PT sample. We found that the ferroelectric poling induces an in-plane compressive strain which is transferred to the film, thus giving rise to a reduction in the in-plane tensile strain of the LBMO film. As a result, the resistivity is reduced while the magnetoresistance (MR), ferromagnetism, and T_C are enhanced. The analysis of the results show that the reduction in the lattice distortion of MnO_6 octahedra induced by ferroelectric poling plays a crucial role in understanding the strain effects in LBMO films.

II. EXPERIMENTAL DETAILS

We have grown the PMN-PT single crystals by a modified Bridgman technique. The crystals were cut into small plates ($10 \times 2.5 \times 0.5 \text{ mm}^3$) with the plate normal in the $\langle 001 \rangle$ crystal direction and polished to a surface roughness less than 1 nm. LBMO films were deposited on the (001)-oriented and polished PMN-PT substrates using dc magnetron sputtering.¹¹ The deposition was carried out in an argon-oxygen flow with 60% Ar and 40% O_2 at a pressure of 5 Pa

^{a)}Electronic mail: zrk@ustc.edu.

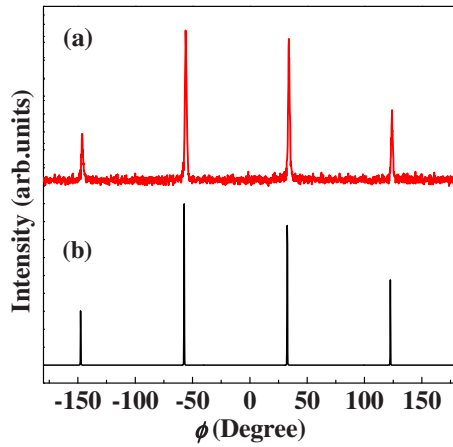


FIG. 1. (Color online) XRD ϕ scans on the (a) LBMO(101) and (b) PMN-PT(101) reflections.

and a substrate temperature of 700 °C. After deposition, the films were cooled to room temperature and postannealed in 1 atm of flowing O₂ at 700 °C for 30 min using a rapid thermal processor furnace. Although the lattice constants ($a \sim b \sim c \sim 4.02$ Å) of the PMN-PT substrate are larger than those [$a \sim b \sim c \sim 3.902$ Å (Ref. 12)] of the LBMO bulk material, recent work by Thiele *et al.*¹³ and Zheng *et al.*^{11,14} demonstrate that it is still possible to epitaxially grow manganite thin films on PMN-PT substrates. X-ray diffraction (XRD) θ - 2θ scan on the LBMO/PMN-PT structure¹⁴ and ϕ scans on LBMO(101) and PMN-PT(101) reflections (see Fig. 1) using a Bruker D8 Discover x-ray diffractometer indicate that LBMO films were epitaxially grown on PMN-PT substrates.

The resistivity of the LBMO film was measured using the electrical measurement circuit^{11,14} shown in the inset (a) of Fig. 3. Since the resistance ($\sim 6.9 \times 10^4$ Ω) of the conducting LBMO film at room temperature is much smaller than that ($\sim 3 \times 10^9$ Ω) of the PMN-PT substrate, the LBMO film in fact serves as the top electrode for poling the PMN-PT substrate. This was achieved by applying a dc poling field E (+10 kV/cm) to the LBMO/PMN-PT structure through the LBMO film (top electrode) and bottom gold electrode using a Keithley 6517A electrometer. Magnetic measurements were performed with a superconducting quantum interference device magnetometer (SQUID-7T, Quantum Design) with the magnetic field applied parallel to the film plane.

III. RESULTS AND DISCUSSION

Figure 2 shows the temperature dependence of the resistivity for the LBMO film when the PMN-PT substrate is in the unpoled state (referred to as P_r^0) and positively poled state (i.e., electric dipole moments point to the LBMO film, referred to as P_r^+), respectively. For P_r^0 state, the resistivity of the film increases with decreasing temperature and shows an appreciable insulator-to-metal-like transition near $T_{MI} \sim 146$ K, which can be more clearly seen from the $\ln \rho$ versus $T^{-1/4}$ curves shown in the inset (a) of Fig. 2. After the measurements of the resistivity as a function of temperature for P_r^0 state, we *in situ* poled the PMN-PT substrate by ap-

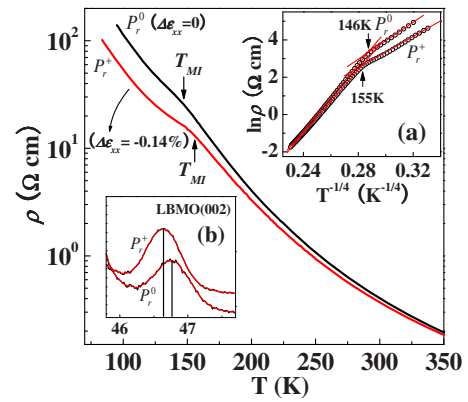


FIG. 2. (Color online) Temperature dependence of the resistivity for the LBMO film when the PMN-PT substrate is in P_r^0 and P_r^+ state, respectively. The inset (a) and (b) show the $\ln \rho$ vs $T^{-1/4}$ curves and the XRD patterns of the LBMO(002) reflections for P_r^0 and P_r^+ state, respectively.

plying an electric field of +10 kV/cm to the LBMO/PMN-PT structure at room temperature and turned off the poling field after 15 min. Since the PMN-PT substrate has a ferroelectric Curie temperature of ~ 155 °C (much higher than room temperature), the polarization direction will remain toward the poling direction after the poling field has been turned off. It can be seen that, associated with the switch of the poling state from P_r^0 to P_r^+ , the resistivity decreases noticeably in the whole temperature range and T_{MI} shifts to a higher temperature by ~ 9 K. *In situ* XRD measurements indicate that, associated with the poling of the PMN-PT substrate, the 2θ value of the LBMO(002) reflection shifts from 46.79° to 46.65° [inset (b) of Fig. 2], corresponding to an increase in the lattice constant c from ~ 3.883 to 3.894 Å. Therefore, the out-of-plane compressive strain ε_{zz} [$\varepsilon_{zz} = (c_{\text{film}} - c_{\text{bulk}}) / c_{\text{bulk}}$] is reduced from -0.49% to -0.21% (i.e., $\Delta\varepsilon_{zz} = 0.28\%$). Assuming approximate volume preserving distortion, an increase in ε_{zz} by 0.28% would be accompanied by a decrease in the in-plane tensile strain ε_{xx} by 0.14% (i.e., $\Delta\varepsilon_{xx} = -0.14\%$) using the expression $\Delta\varepsilon_{zz} = -2\nu / (1 - \nu) \Delta\varepsilon_{xx}$ where ν ($=0.5$) is the Poisson's ratio. Such a decrease in the in-plane tensile strain would reduce the tetragonal distortion of MnO₆ octahedra of the film, as recently revealed by the angular resolved x-ray absorption spectroscopy study of epitaxially strained La_{0.7}Sr_{0.3}MnO₃ thin films by Souza-Neto *et al.*,¹⁵ and thus weakens the electron-lattice coupling strength, as pointed out by Millis *et al.*¹⁶ As a result, the itinerancy of the e_g electrons would be enhanced, giving rise to a decrease in the resistivity of the LBMO film.

Figure 3 shows the temperature dependence of the field-cooled magnetization of the LBMO film for P_r^0 and P_r^+ state, respectively. With decreasing temperature, the magnetization shows a sharp increase near 150 K, which coincides with T_{MI} , indicating that the insulator-to-metal-like transition near T_{MI} is correlated with this paramagnetic to ferromagnetic (FM) phase transition. Although the magnetic ground state is FM, the LBMO film is an insulator at low temperatures. It is reasonable that there exist hole rich Mn³⁺-O-Mn⁴⁺ ferromagnetically coupled clusters which are embedded in the Mn³⁺-O-Mn³⁺ antiferromagnetically coupled matrix. The double-exchange interaction is operative primarily within the

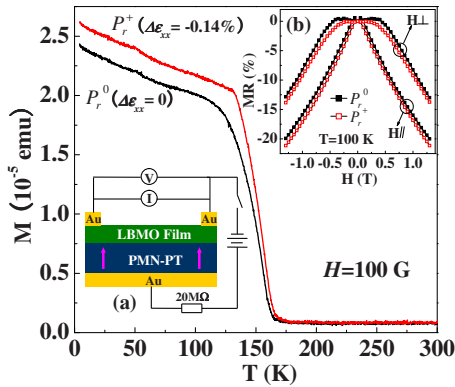


FIG. 3. (Color online) Temperature dependence of the field-cooled magnetization for the LBMO film when the PMN–PT substrate is in P_r^0 and P_r^+ state, respectively. The inset (a) shows a schematic diagram of the LBMO/PMN–PT structure and the circuit for electrical measurement. The arrow represents the poling direction. The inset (b) shows MR of the film at 100 K as a function of the magnetic field applied parallel (or perpendicular) to the film plane for P_r^0 and P_r^+ state, respectively.

FM clusters while the long-range antiferromagnetic (AFM) order in the host lattice is supported predominantly by the $\text{Mn}^{3+}\text{--O--Mn}^{3+}$ exchange coupling which is weaker than the $\text{Mn}^{3+}\text{--O--Mn}^{4+}$ double-exchange interaction.¹⁷ Because the concentration of FM clusters is not high enough, they do not interact with one another, thereby giving rise to the FM insulating behavior of the resistivity at low temperatures. Associated with the establishment of FM ordering within FM clusters below T_C (~ 150 K), faster hopping of e_g electrons within FM clusters is expected, which could lead to the insulator-to-metal-like transition near T_{MI} . We note that, associated with the switch of the poling state from P_r^0 to P_r^+ , both ferromagnetism and T_C are clearly enhanced. At 4.2 K, the magnetization was enhanced by $\sim 8.2\%$. As discussed above, a decrease in the in-plane tensile strain weakens the electron-lattice coupling and enhances the electron hopping amplitude.¹⁶ The enhanced electron hopping would increase the ferromagnetism of the FM clusters since the FM double-exchange interaction needs active hopping of electrons between Mn^{3+} and Mn^{4+} ions. On the other hand, the enhanced ferromagnetism within FM clusters cants the surrounding spins in the AFM matrix toward the same direction of the FM clusters because of an interface superexchange interaction,¹⁸ which could also contribute to the enhancement of the ground state ferromagnetism of the film.

The ferroelectric-poling-induced reduction in the in-plane tensile strain also influences MR of the LBMO film. The inset (b) of Fig. 3 shows MR of the film at $T=100$ K as a function of magnetic fields applied parallel (or perpendicular) to the film plane for P_r^0 and P_r^+ state, respectively. Here, MR is defined as $\text{MR} = [\rho(0) - \rho(H)] / \rho(0)$ where $\rho(0)$ and $\rho(H)$ are the resistivity of the LBMO film in zero magnetic field and a magnetic field H , respectively. Whether the magnetic field is applied parallel or perpendicular to the film plane, associated with the reduction in the in-plane tensile strain, MR of the film is enhanced appreciably. It is noted that similar strain-induced enhancement of MR has been observed in the $\text{La}_{0.7}\text{Ba}_{0.3}\text{MnO}_3$ films epitaxially grown on PMN–PT substrates.¹¹ The underlying mechanism that is re-

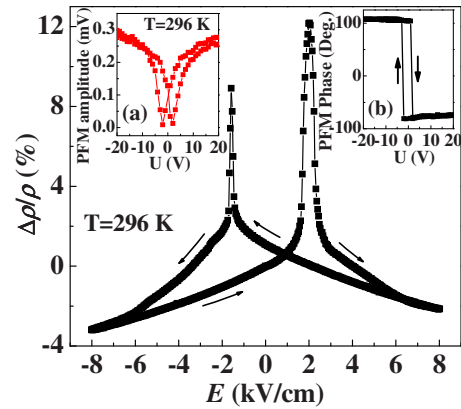


FIG. 4. (Color online) Relative change in the resistivity of the LBMO film as a function of electric field applied to the PMN–PT substrate through the top and bottom electrodes. The inset (a) and (b) show the amplitude and phase of the PFM signal as a function of electric potential applied to the PMN–PT single crystal, respectively.

sponsible for the enhancement of MR for the LBMO/PMN–PT structure is probably the same as that for the $\text{La}_{0.7}\text{Ba}_{0.3}\text{MnO}_3$ /PMN–PT structure. Namely, the effects of the induced strain on MR can be explained in terms of strain-induced modification of phase separation. At 100 K, the film is in FM insulating state. That is, FM metallic clusters are embedded in the AFM insulating matrix with the volume fraction of the latter dominating over that of the former. Associated with the reduction in the in-plane tensile strain, the volume fraction of the FM metallic phase increases at the expense of the AFM insulating phase (as reflected by the decrease in the resistivity and the increase in magnetization and T_C). Consequently, MR of the film increases due to enhanced volume fraction of FM metallic phase.

Figure 4 shows the relative change in the resistivity of the LBMO film as a function of bipolar electric field applied to the PMN–PT substrate. The resistivity-electric field (ρ - E) hysteresis loop shows a butterflylike shape with the resistivity change exhibiting the same sign for opposite directions of applied electric field. This is a typical behavior of the resistivity change due to the strain induced by the reversal of the polarization direction in the PMN–PT substrate.¹³ If the ferroelectric field effect plays a dominant role in influencing the resistivity, one would observe a rectanglelike ρ - E hysteresis loop with the resistivity change exhibiting opposite signs for opposite directions of applied electric field, as previously observed in the $\text{La}_{1-x}\text{Ba}_x\text{MnO}_3$ ($x=0.1, 0.15$)/ $\text{Pb}(\text{Zr}_{0.2}\text{Ti}_{0.8})\text{O}_3$ structures.¹⁹ Thus, the butterflylike ρ - E hysteresis loop gives further evidence that the strain induced by poling plays a dominant role in influencing the transport properties of the LBMO film while the ferroelectric field effect is minor and negligible. Measurements of piezoresponse force microscopy (PFM) on a PMN–PT single crystal using a scanning probe microscope operated in the piezoforce mode showed that the amplitude of the PFM signal (which is in proportional to the induced out-of-plane strain) also exhibits butterflylike hysteresis loop [inset (a) of Fig. 4], which gives direct evidence that the modulation of the resistivity is strain-induced and is resulted from the electric-field-induced reversal of the polarization

direction of ferroelectric domains in the PMN–PT substrate. As can be seen in the inset (b) of Fig. 4, with the change of the electric potential in the sequence of $0 \rightarrow -20 \text{ V} \rightarrow +20 \text{ V} \rightarrow 0 \text{ V}$, the polarization direction of ferroelectric domains rotates by 180° , as reflected by the 180° change in the PFM phase, giving evidence that the strain induced by the polarization reversal is responsible for the resistivity modulation.

IV. CONCLUSIONS

In summary, we have studied the effects of ferroelectric-poling-induced strain on the transport and magnetic properties of lightly doped $\text{La}_{7/8}\text{Ba}_{1/8}\text{MnO}_3$ thin films epitaxially grown on ferroelectric PMN–PT substrates. The ferroelectric poling *in situ* reduces the in-plane tensile strain of the film, giving rise to a decrease in the resistivity and an increase in the Curie temperature, ferromagnetism, and MR of the film. We discussed these strain effects within the framework of the phase separation which is significantly influenced by the strain induced by ferroelectric poling. The results also demonstrate that the strain induced by ferroelectric poling play a dominant role in influencing the transport and magnetic properties of the film while the ferroelectric field effect is minor and negligible in the LBMO/PMN–PT structure.

ACKNOWLEDGMENTS

This work was supported by the Hong Kong Research Grants Council under Grant No. CERG PolyU 5122/07E,

and the Center for Smart Materials of the Hong Kong Polytechnic University.

- ¹J. Zhang, H. Tanaka, T. Kanki, J. H. Choi, and T. Kawai, *Phys. Rev. B* **64**, 184404 (2001).
- ²X. J. Chen, S. Soltan, H. Zhang, and H.-U. Habermeier, *Phys. Rev. B* **65**, 174402 (2002).
- ³M. Ziese, H. C. Semmelhack, and K. H. Han, *Phys. Rev. B* **68**, 134444 (2003).
- ⁴S. W. Jin, G. Y. Gao, Z. Z. Yin, Z. Huang, X. Y. Zhou, and W. B. Wu, *Phys. Rev. B* **75**, 212401 (2007).
- ⁵T. Wu, S. B. Ogale, S. R. Shinde, A. Biswas, T. Polletto, R. L. Greene, T. Venkatesan, and A. J. Millis, *J. Appl. Phys.* **93**, 5507 (2003).
- ⁶T. Kanki, T. Yanagida, B. Vilquin, H. Tanaka, and T. Kawai, *Phys. Rev. B* **71**, 012403 (2005).
- ⁷P. Murugavel, T. W. Noh, and J. G. Yoon, *J. Appl. Phys.* **95**, 2536 (2004).
- ⁸P. Murugavel, J. H. Lee, K. B. Lee, J. H. Park, J. S. Chung, J. G. Yoon, and T. W. Noh, *J. Phys. D: Appl. Phys.* **35**, 3166 (2002).
- ⁹P. Murugavel, J. H. Lee, J. G. Yoon, T. W. Noh, J.-S. Chung, M. Heu, and S. Yoon, *Appl. Phys. Lett.* **82**, 1908 (2003).
- ¹⁰P. Orgiani, A. Guarino, C. Aruta, C. Adamo, A. Galdi, A. Yu. Petrov, R. Savo, and L. Maritato, *J. Appl. Phys.* **101**, 033904 (2007).
- ¹¹R. K. Zheng, Y. Jiang, Y. Wang, H. L. W. Chan, C. L. Choy, and H. S. Luo, *Phys. Rev. B* **79**, 174420 (2009).
- ¹²P. Mandal and B. Ghosh, *Phys. Rev. B* **68**, 014422 (2003).
- ¹³C. Thiele, K. Dörr, S. Fähler, L. Schultz, D. C. Meyer, A. A. Levin, and P. Paufler, *Appl. Phys. Lett.* **87**, 262502 (2005).
- ¹⁴R. K. Zheng, Y. Wang, H. L. W. Chan, C. L. Choy, and H. S. Luo, *Appl. Phys. Lett.* **92**, 082908 (2008).
- ¹⁵N. M. Souza-Neto, A. Y. Ramos, H. C. N. Tolentino, E. Favre-Nicolin, and L. Ranno, *Phys. Rev. B* **70**, 174451 (2004).
- ¹⁶A. J. Millis, T. Darling, and A. Migliori, *J. Appl. Phys.* **83**, 1588 (1998).
- ¹⁷J. Töpfer and J. B. Goodenough, *Chem. Mater.* **9**, 1467 (1997).
- ¹⁸M. Muroi and R. Street, *Aust. J. Phys.* **52**, 205 (1999).
- ¹⁹T. Kanki, Y.-G. Park, H. Tanaka, and T. Kawai, *Appl. Phys. Lett.* **83**, 4860 (2003).